Progress and challenges with local approaches to cleavage fracture

DOI:
10.1016/j.prostr.2020.01.060

Document Version
Final published version

Available online at www.sciencedirect.com

ScienceDirect

Procedia Structural Integrity 23 (2019) 39–44

Structural Integrity Procedia

www.elsevier.com/locate/procedia

9th International Conference on Materials Structure and Micromechanics of Fracture

Progress and challenges with local approaches to cleavage fracture

A.P. Jivkov[a,*], M. Ford[a,b], M. Yankova[a], D. Sarzosa[c], C. Ruggieri[c]

[a]*Mechanics and Physics of Solids Research Group, School of MACE, The University of Manchester, Manchester M13 9PL, UK*
[b]*Wood, Birchwood Park, Warrington WA3 6AE, UK*
[c]*Department of Naval Architecture and Ocean Engineering, University of Sao Paulo, Sao Paulo, Brazil*

Abstract

Local approaches (LA) to cleavage fracture incorporate microstructure information and failure mechanisms into mathematical models for calculation of component failure probability. They offer a promising mechanistic alternative to global approaches and have been successfully applied to predict cleavage fracture toughness (CFT) changes due to material degradation and geometry effects. Predicting the dependence of CFT on temperature, specifically in the ductile-to-brittle transition (DBT) regime, remains a challenge. This work offers one avenue for addressing the challenge by revisiting the mathematical basis of LA and demonstrating that changes in continuum mechanical fields due to changes of deformation properties with temperature are insufficient to deliver predictions in agreement with experimentally measured CFT dependence on temperature. This suggests that the process by which cleavage initiators are generated is dependent on temperature separately from the dependence of the deformation properties on temperature. The temperature dependence of the generation process is derived for the material studied in the work. A methodology is described for predicting CFT in the DBT regime, using deformation and fracture toughness properties at one temperature and deformation properties at any other temperature of interest.

Keywords: Ferritic steels; Cleavage fracture; Ductile-to-brittle transition; Local approach

1. Introduction

The ability to predict changes of cleavage fracture toughness (CFT) with temperature, crack geometry and material degradation is critical to safety assessment and life extension of structural components. Global approaches to integrity

* Corresponding author. *Tel.*: +44-161-306-3765; *E-mail:* andrey.jivkov@manchester.ac.uk

10.1016/j.prostr.2020.01.060

assessment, such as those based on the failure assessment diagram, are overly conservative without explicit knowledge of CFT values for every material state and crack geometry, i.e. without extensive testing, which is not feasible in most cases. Local approaches (LA) to cleavage fracture are considered to be a promising mechanistic alternative to global approaches. These have been developed over the last 35 years with the view to incorporate microstructure information and failure mechanisms. A recent review by Ruggieri and Dodds (2018) covers the LA achievements in predicting changes of CFT due to geometry effects. A modified LA to address changes of CFT due to material degradation has also been proposed by Jivkov et al. (2019). Predicting the dependence of CFT on temperature, specifically in the ductile-to-brittle transition (DBT) regime, while researched extensively, e.g. Kotrechko et al. (2007), remains a challenge for existing LA. This work addresses the challenge.

2. Methodology

2.1. Material

Material under consideration is 22NiMoCr37 ferritic steel, for which the deformation and cleavage fracture toughness (CFT) properties at a number of temperatures within the lower shelf and in DBT are readily available. The reference temperature for this material is between -104°C and -110°C. Data at three temperatures, T_k, are used in this work. Deformation behaviour is modelled with an elastic-power law hardening, with Young's modulus, E, proportionality stress, σ_0, and Hollomon hardening exponent, n, derived from experimental data at each T_k. The CFT values, J_c, were obtained with standard C(T) specimens, W = 50 mm, B,b = 25 mm. Maximum likelihood method is used to test that J_c follow two-parameter Weibull distributions and to determine the characteristic CFT, J_0, i.e. the value at which the probability of cleavage is 0.632. Deformation properties and J_0 at T_k are given in Table 1. All J_c values are shown in Fig. 4 together with modeling predictions. Notably, the values suggest that all failures occurred under plane strain small scale yielding as prescribed by the ASTM standards: $B,b > 25(J_c/\sigma_0)$.

Table 1. Deformation properties and characteristic toughness of the material at the analysed temperatures

T_k	E [MPa]	σ_0 [MPa]	σ_{UTS} [MPa]	n	J_0 [N/mm]
T_1 = -154°C (119 K)	219860	768.3	882.0	14.405	7.65
T_2 = -91°C (182 K)	214190	594.9	727.2	11.970	57.6
T_3 = -40°C (233 K)	209600	520.4	679.1	10.090	235.3

2.2. Finite element analyses

Boundary layer models (BLM) with finite crack tip radii are used to establish the stress and strain fields with finite strain analyses and calculate cleavage crack driving forces described in the next sub-section. The use of BLM is justified by the conditions under which experimental CFT values were obtained. Results presented in this work are calculated with initial crack tip radii r_k = 0.5, 5, 10, and 20 μm for the corresponding T_k. These are selected to follow closely the crack tip opening displacements determined with small strain analysis of BLM with sharp tips. Maximum principal stress and equivalent plastic strain profiles ahead of the crack are shown in Fig. 1 for future reference in the discussion. Analyses of models with smaller (half) and larger (double) radii were also performed to assess the effect of selection on the cleavage crack driving forces. It was found that this effect is negligible.

2.3. Cleavage crack driving force

Cleavage fracture can be viewed as an inhomogeneous spatial Poisson point process, with points corresponding to cleavage initiators (CI). Such processes have intensity function $\lambda(\boldsymbol{x})$ representing the probability of finding a point within an infinitesimal volume located at $\boldsymbol{x}$. The integral of $\lambda(\boldsymbol{x})$ over a bounded region V, denoted by $\Lambda(V)$, multiplied by the volume density of points, represented by $1/V_0$, gives the expected number of points in V. The probability of finding a point in V is $p(V)$=1-exp[-$\Lambda(V)/V_0$].

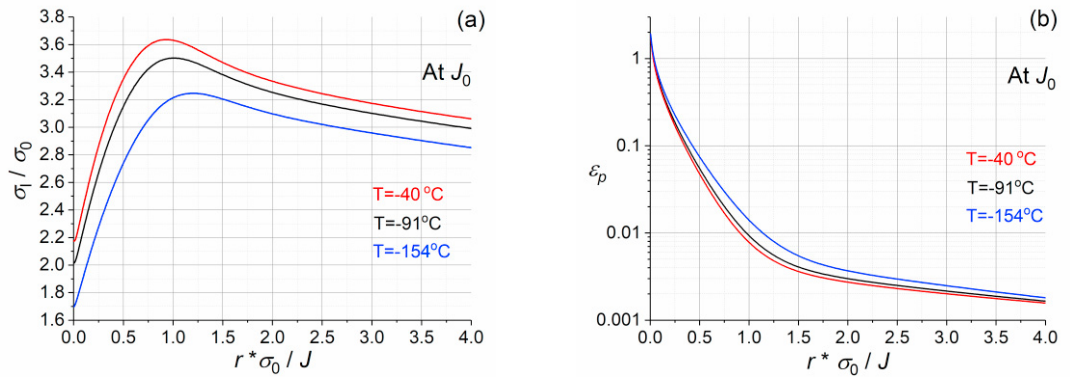

Fig. 1. (a) Normalised maximum principal stress and (b) equivalent plastic strain obtained with r_k at $J_{0,k}$.

CI form at second-phase particles with intensity depending on several conditions. A particle at location $\boldsymbol{x}$ may deform together with the surrounding matrix, form a void by detaching from the matrix or by breaking and blunting, or break and form a sharp micro-crack. The last mechanism creates eligible micro-cracks with size distribution approximated by a power law *f(a)* given in Eq. (1) with scale a_0, shape β, and size density ρ. CI are eligible micro-cracks larger than a critical size $a_c > a_0$, and their intensity is $\lambda(a_c)$ in Eq. (1). It is reasonable to assume that CI populations formed at different temperatures in the same material have the same a_0 and β but potentially different size densities, because they originate from identical particle size distributions. This leads to an intensity function, $\lambda(\boldsymbol{x})$, for all populations with the same a_0 and β, given also in Eq. (1). The non-dimensional $\theta(\boldsymbol{x})$ is a position dependent thinning function for the Poisson point process, measuring the number of CI in the infinitesimal volume at $\boldsymbol{x}$ relative to some reference number. CI populations with different power law parameters are possible, and this will be mentioned in the discussion section.

$$f(a)=\rho\left(\frac{a_0}{a}\right)^{\beta};\qquad \lambda(a_c)=\int_{a_c}^{\infty} f(a)da=\rho\frac{a_0}{\beta-1}\left(\frac{a_0}{a_c}\right)^{\beta-1};\qquad \lambda(\mathrm{x})=\theta(\mathrm{x})\left(\frac{a_0}{a_c}\right)^{\beta-1} \tag{1}$$

$$a_c=\frac{\pi E\gamma}{2\left(1-\nu^2\right)\sigma_1^2};\qquad \lambda(\mathrm{x})=\theta(\mathrm{x})\left(\frac{\sigma_1}{\sigma_u}\right)^{2\beta-2};\qquad \sigma_u=\left(\frac{\pi E\gamma}{2\left(1-\nu^2\right)a_0}\right)^{1/2}. \tag{2}$$

$$P_f(\sigma_w)=1-\exp\left(\frac{\sigma_w}{\sigma_u}\right)^m;\qquad \sigma_w=\left(\frac{1}{V_0}\int_V\theta(\mathrm{x})\sigma_1^m dV\right)^{1/m} \tag{3}$$

The critical micro-crack size, a_c, is calculated from a criterion for unstable growth, e.g. for a penny-shaped crack this is given in Eq. (2), where E and ν are Young's modulus and Poisson's ratio, respectively, σ_1 is the maximum principal stress at location $\boldsymbol{x}$, and γ is a measure of fracture energy. This leads to CI intensity $\lambda(\boldsymbol{x})$ given in Eq. (2) with scaling stress σ_u. The expected number of CI in a region V is proportional to $\Lambda(V)$, i.e. integral of $\lambda(\boldsymbol{x})$ over V. By introducing $m=2\beta-2$, this is converted to the known expression for probability of cleavage, P_f, given in Eq. (3) with a Weibull stress, σ_w, considered as a cleavage crack driving force. Typical application of the Weibull-stress-based probability involves calibration of m and σ_u with experimentally measured failure probabilities. Options for the thinning function used in past works include $\theta(\boldsymbol{x})=H(\varepsilon_p)$, where $H(\varepsilon_p)$ is the Heaviside function of the equivalent plastic strain at $\boldsymbol{x}$, e.g. in Mudry (1987) and $\theta(\boldsymbol{x})=1-\exp(-\lambda\varepsilon_p)$, where λ is a further fitting parameter, e.g. in Ruggieri et al. (2015). The latter form of the thinning function will be used in this work.

3. Results and discussion

Figure 2 shows the dependence of the Weibull stress on the parameter m. The Weibull stress is calculated with $\lambda = 1$ in $\theta(\boldsymbol{x})$ and scaled with the material flow stress, σ_f, for each T_k. The curves are obtained at J_0 for the corresponding T_k, but the relations between the curves are the same for any other selected toughness percentile and any constant λ across temperatures. When a constant scaling volume is used across temperatures (Fig. 2a), the curves do not intersect within the practical m-interval considered. This suggests that a calibration of m, similar to the one used between different constraint conditions, is not feasible for the temperature dependence. Several options could be considered. Firstly, a constant m could be assumed, requiring temperature dependence of σ_u for fracture toughness predictions. This approach has been taken e.g. by Petti and Dodds (2005). Secondly, it is possible to assume that σ_u is proportional to σ_f, requiring temperature dependence of m. This has been considered e.g. by Cao at al. (2011). Both these options are viable and in essence they require that independent CI populations are generated in the same material at different temperatures. There is no experimental evidence to support either option, and an alternative approach is proposed here.

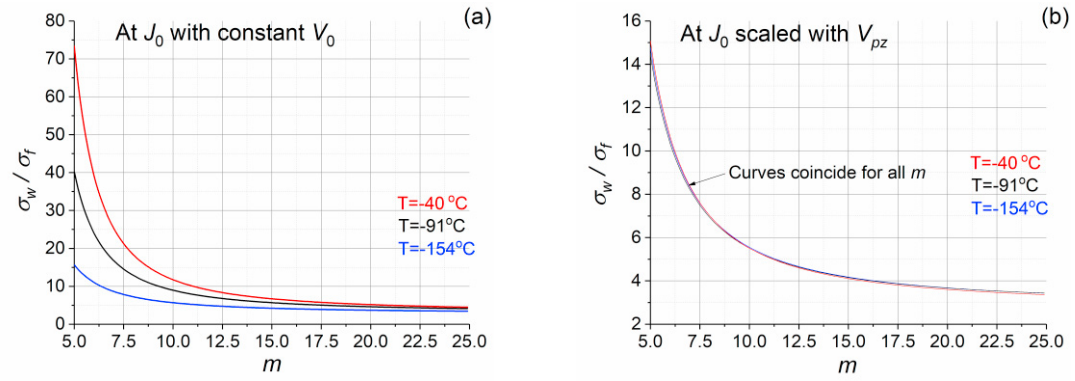

Fig. 2. Normalised Weibull stress dependence on m calculated with: (a) constant scaling volume and (b) plastic zone volume.

When the Weibull stress is calculated with a scaling volume equal to the current plastic zone volume, the curves coincide as shown in Fig. 1(b). While this is not a physical scaling, it demonstrates that the number of CI in the plastic zone at given percentile toughness, J_p, is the same for all temperatures. Required is an appropriate $\theta(\boldsymbol{x})$ to reflect this observation – for temperatures $T_i > T_j$, the toughness percentiles are $J_p(T_i) > J_p(T_j)$ and since the plastic zone volumes scale with J^2, $V_{pz}(T_i) >> V_{pz}(T_j)$, but contain the same number of CI. Finding such $\theta(\boldsymbol{x})$ will allow fracture toughness predictions in DBT to be made with arbitrary m (potentially determined with two constraint conditions at a single temperature) and σ_u proportional to the corresponding σ_f. The stress and strain profiles shown in Fig.1 give an indication that the differences on the mechanical fields due to changed deformation behaviour with temperature are relatively small. This does not allow for constructing a thinning function with the required behaviour based solely on the stress and strain fields.

By comparing numbers of CI generated in the plastic zones at different temperatures and at different toughness percentiles the function shown in Eq. (4) is proposed. Note that T is in Kelvin (given in Table 1), and that the parameters of the scale $\lambda(T)$ are specific to the studies material.

$$\theta(\mathrm{x}) = 1 - \exp\left[-\lambda(T)\varepsilon_p(\mathrm{x})\right]; \qquad \lambda(T) = \exp\left(-12 + \frac{2250}{T}\right), T[K] \tag{4}$$

The Weibull stress histories obtained with the proposed thinning function are presented in Fig. 3. It is assumed here that the material has been tested at T=-91°C and the process of predicting the toughness at the lower (Fig. 3a) and higher (Fig. 3b) temperatures is illustrated. The results show an excellent agreement with experimentally measured characteristic CFT values. The toughness of both the very low and the very high, well within the DBT region, temperatures are only slightly underpredicted. In practice, the prediction process requires accurate measurement of

the CFT distribution at one temperature in the DBT regime. Numerical analysis following the proposed scheme will provide the Weibull stress history and specifically the factor $\sigma_u/\sigma_f = \sigma_w(J_0)/\sigma_f$. For any other temperature, the deformation properties are only required. Numerical analysis at that temperature following the proposed scheme will provide the Weibull stress history to predict the corresponding J_0 as the value at which the same factor is reached.

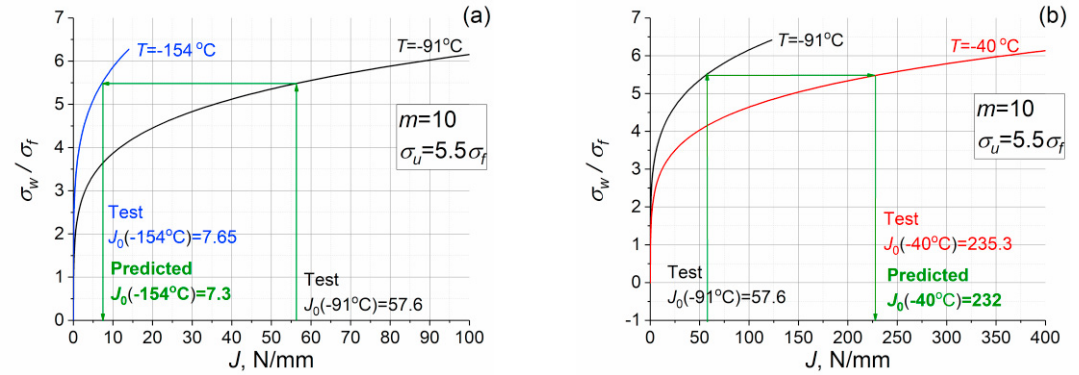

Fig. 3. Predictions of characteristic CFT at (a) lower and (b) higher temperatures with known data at a single temperature.

The model predictions for the probability of failure at the three temperatures are shown in Fig. 4 (thicker lines) together with the experimental CFT data points (symbols) presented with median-ranked probabilities. In addition the maximum likelihood (ML) estimates for the characteristic toughness (also shown in Table 1) and shape are given, and the correspondingly derived curves based on Weibull distribution of J with these parameters (thinner lines). It can be seen that the model makes very good estimations of the CFT distribution, particularly at the temperatures above T_0 (Figs. 4b and 4c), where the model and ML estimates practically coincide and follow closely the experimental data. At the very low temperature the prediction is still reasonable, considering the large temperature gap bridged by the model. Notably, the experimental data does not follow the requirement for the shape of the Weibull distribution of J to be close to 2, which suggests that in some of the tests cleavage might have initiated by a mechanism different from the one described here - crack propagation from micro-crack formed by rupture of second-phase particle due to plastic overload. One possibility is cleavage initiation from small existing defects, the presence of which is not captured by the presented LA.

4. Conclusions

By revisiting the mathematical basis for the local approaches to cleavage fracture, and analyzing an appropriate set of deformation and fracture toughness data, it has been shown that the use of the stress and strain fields ahead of a microscopic crack is not sufficient to deliver an LA formulation that can predict the toughness variation in the ductile-to-brittle transition regime. It has been demonstrated that the number of cleavage initiators within the plastic zone ahead of the crack is constant at given toughness percentile across temperatures, which provides a reference point for developing a thinning function, i.e. a function prescribing how many cleavage initiators must be generated relative to a reference case (for example all particles). A thinning function, based on the known exponential dependence on the equivalent plastic strain and a fitted dependence of its scale on temperature has been proposed. The parameters given in Eq. (4) are specific to the studied material and need to be further confirmed for this material at other temperatures. Expressions of similar type could be tested with other materials and possibly re-calibrated. Very good agreements between the experimental data and the results obtained with the proposed model have been shown, both in predicting the characteristic cleavage fracture toughness and the probability of failure. Critical further work is to investigate and explain the reason for the very significant effect of temperature on the conversion of second-phase particles into cleavage initiators, expressed by the exponential dependence of λ on T in Eq. (4).

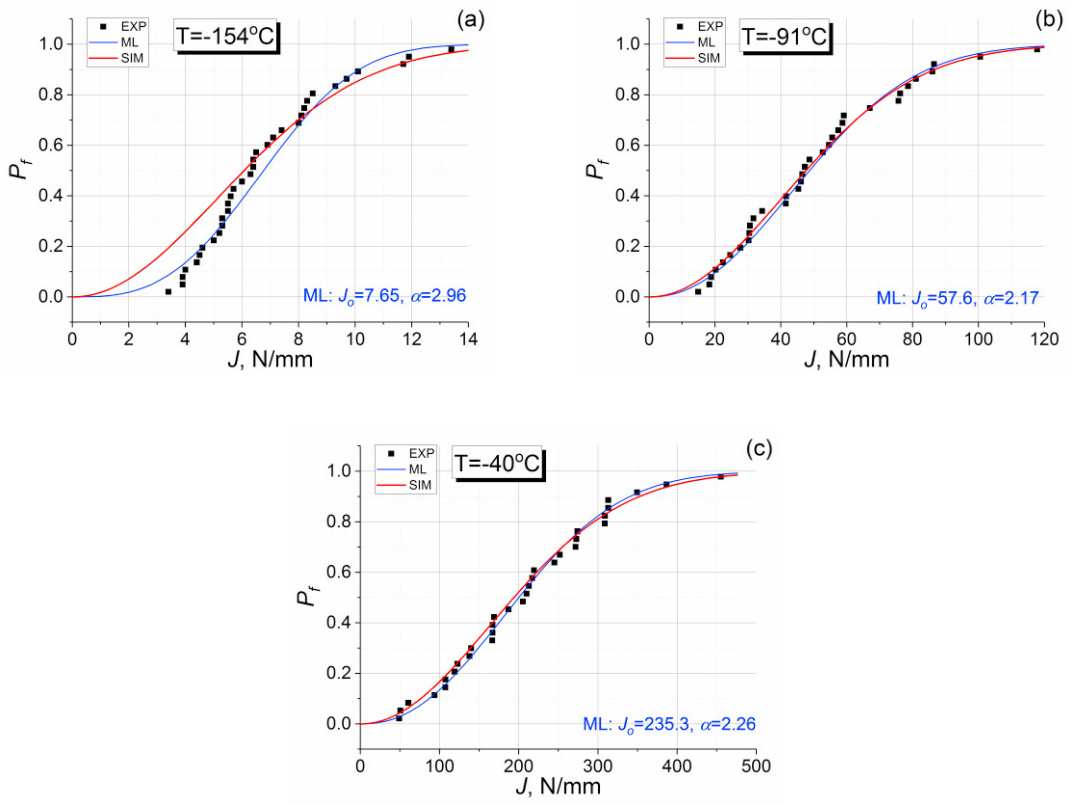

Fig. 4. Probability of failure at studied temperatures predicted by the model in comparison with the experimental data and estimations based on the maximum likelihood method.

Acknowledgements

Jivkov acknowledges gratefully the financial support of EPSRC via grant EP/N026136/1.

References

Cao, Y., Hui, H., Wang, G., Xuan, F-Z, 2011. Inferring the temperature dependence of Beremin cleavage model parameters from the Master Curve. Nuclear Engineering & Design 241, 39–45.

Jivkov, A.P., Sarzosa Burgos, D., Ruggieri, C., Beswick, J., Savioli, R., James, P., Sherry, A., 2019. Use of local approaches to calculate changes in cleavage fracture toughness due to pre-straining and constraint effects. Theoretical and Applied Fracture Mechanics, to appear.

Kotrechko, S., Strnadel, B., Dlouhy, I., 2007. Fracture toughness of cast ferritic steel applying local approach. Theoretical and Applied Fracture Mechanics 47, 171-181.

Mudry, F., 1987. A local approach to cleavage fracture. Nuclear Engineering & Design 105, 65–76.

Petti, J.P., Dodds Jr., R.H., 2005. Calibration of the Weibull stress scale parameter, σ_u, using the Master Curve. Engineering Fracture Mechanics 72, 91-120.

Ruggieri, C., Dodds Jr., R.H., 2018. A local approach to cleavage fracture modelling: an overview of progress and challenges for engineering applications. Engineering Fracture Mechanics 187, 381-403.

Ruggieri, C., Savioli, R., Dodds Jr., R.H., 2015. An engineering methodology for constraint corrections of elastic-plastic fracture toughness – Part II: Effects of specimen geometry and plastic strain on cleavage fracture predictions. Engineering Fracture Mechanics 146, 185-209.